Published online 2 September 2009

Nucleic Acids Research, 2009, Vol. 37, No. 19 ***6389–6399***
doi:10.1093/nar/gkp695

The yeast high mobility group protein HMO2, a subunit of the chromatin-remodeling complex INO80, binds DNA ends

Sreerupa Ray and Anne Grove*

Department of Biological Sciences, Louisiana State University, Baton Rouge, LA 70803, USA

Received April 3, 2009; Revised June 21, 2009; Accepted August 7, 2009

ABSTRACT

DNA damage is a common hazard that all cells have to combat. *Saccharomyces cerevisiae* HMO2 is a high mobility group protein (HMGB) that is a component of the chromatin-remodeling complex INO80, which is involved in double strand break (DSB) repair. We show here using DNA end-joining and exonuclease protection assays that HMO2 binds preferentially to DNA ends. While HMO2 binds DNA with both blunt and cohesive ends, the sequence of a single stranded overhang significantly affects binding, supporting the conclusion that HMO2 recognizes features at DNA ends. Analysis of the effect of duplex length on the ability of HMO2 to protect DNA from exonucleolytic cleavage suggests that more than one HMO2 must assemble at each DNA end. HMO2 binds supercoiled DNA with higher affinity than linear DNA and has a preference for DNA with lesions such as pairs of tandem mismatches; however, comparison of DNA constructs of increasing length suggests that HMO2 may not bind stably as a monomer to distorted DNA. The remarkable ability of HMO2 to protect DNA from exonucleolytic cleavage, combined with reports that HMO2 arrives early at DNA DSBs, suggests that HMO2 may play a role in DSB repair beyond INO80 recruitment.

INTRODUCTION

All organisms depend on efficient repair of DNA double strand breaks (DSBs) to maintain genomic stability (1,2). The most accurate repair pathway is homologous recombination (HR), which is mainly active during S and G2 as it depends on the presence of sister chromatids, while the more error prone non-homologous end-joining (NHEJ) is active throughout the cell cycle (2). Both repair pathways must negotiate DNA that is packaged into chromatin, and chromatin remodeling is therefore critical to DNA repair (3–7).

The ATP-dependent chromatin remodeling complex INO80 has been recently shown to participate in DSB repair in yeast (3,8–11). The INO80 complex is recruited to the DSB by interaction with the damage-induced phosphorylated histone H2A (γ-H2AX), a phenomenon that requires the high mobility group protein (HMGB) HMO2 (also known as NHP10). HMO2 has been reported to be responsible for interaction with γ-H2AX and its inactivation results in reduced INO80 recruitment to the DSB, but not to impaired chromatin remodeling activity (3). Since H2A phosphorylation is thought to be an early response to DSB formation, INO80—and hence HMO2—may contribute to DSB repair by both pathways.

High mobility group (HMG) proteins are non-histone chromosomal proteins that are classified into three groups, HMGA, HMGB and HMGN depending on their DNA-binding characteristics (12,13). HMGB proteins contain one or more HMG boxes, an ∼80 amino-acid sequence (13,14), and are further classified into two groups depending on sequence specificity; the sequence-specific family consists of transcription factors such as lymphoid enhancer factor (LEF) and sex-determining factor (SRY), while the non-sequence specific family includes HMGB1, HMGB2 and yeast homologs NHP6A and NHP6B (12,14–19). The HMG box is composed of three α-helices which adopt an 'L' shaped fold (14–17,19–21). Binding to the DNA occurs through the minor groove by partial intercalation of hydrophobic amino acids, resulting in DNA bending (12,18,21), and HMGB proteins preferentially bind to distorted DNA such as cisplatin-modified DNA (22,23). HMGB proteins participate in stabilizing chromatin structure and play a role in DNA-dependent processes such as recombination and transcription by facilitating nucleoprotein complex assembly. HMGB proteins have also been suggested to contribute to DNA repair, as evidenced for example by DNA end-joining *in vitro* in the presence of DNA ligase (24–27).

*To whom correspondence should be addressed. Tel: +1 225 578 5148; Fax: +1 225 578 8790; Email: agrove@lsu.edu

Saccharomyces cerevisiae contains 10 HMGB proteins. The single HMG box proteins NHP6A/B participate in transcription by RNA polymerases II and III (18,28–30). HMO1 and HMO2 are more similar to mammalian HMGB proteins by having two HMG-like domains, Box A and Box B. HMO1 has been shown to play a role in plasmid maintenance and normal growth and it also functions in the ribosomal RNA transcription system as well as in regulating ribosomal protein expression (31–36). In the ~25-kDa HMO2, the two domains Box A and Box B are followed by an acidic C-terminal tail in contrast to HMO1, which has a lysine-rich tail. For both HMO1 and HMO2, Box B corresponds to the mammalian Box B while the N-terminal Box A bears little resemblance to mammalian Box A. The HMO1 Box A domain has been shown to contribute to DNA binding and bending (37,38).

We show here that HMO2 binds to DNA ends, both blunt ends and overhangs, and that it protects DNA from exonuclease digestion. Since protection of DNA ends from exonucleolytic cleavage is essential to minimize loss of genetic information before repair can be initiated, and since HMO2 is thought to arrive early at DSBs in its complex with INO80 components, our data suggests that HMO2 may play a role in DSB repair beyond INO80 recruitment.

MATERIALS AND METHODS

Cloning, overexpression and purification of protein

The gene-encoding HMO2 was amplified from yeast genomic DNA using primers NHP10F 5′-CACATAAG CATATGTCAGTTGAA-3′ and NHP10R 5′-CGTCTT ACCATATGTTCAAAGAA-3′ (NdeI sites underlined) and cloned into the NdeI site of pET14b, resulting in expression of HMO2 with an N-terminal His_6-tag. pET14b-HMO2 was transformed into *Escherichia coli* Rosetta Blue and expression of HMO2 was induced by addition of 1 mM isopropyl-β-D-thiogalactopyranoside (IPTG) at A_{600} of 0.2 and induction was carried out for 4 h. Cells were pelleted and then resuspended in lysis buffer pH 7.5 (50 mM $Na_xH_yPO_4$, 300 mM NaCl, 10 mM imidazole, 20% glycerol, 1 mM 2-mercaptoethanol and 1 mM phenylmethylsulfonyl fluoride (PMSF)). Cells were disrupted by sonication. The nucleic acids were digested by adding 2 µl of 2000 U/ml of DNaseI (New England Biolabs) and incubated on ice for 1 h. To the lysate, 0.01% of Triton X-100 was added and the solution was incubated on ice for 1 h and then centrifuged at $6000 \times g$ for 20 min. The lysate was incubated with Ni-NTA agarose beads for 1 h on ice. The nickel beads were equilibrated using lysis buffer prior to use. The beads were washed using wash buffer pH 7.5 (50 mM $Na_xH_yPO_4$, 300 mM NaCl, 20 mM imidazole, 20% glycerol, 1 mM 2-mercaptoethanol and 1 mM PMSF). Proteins were eluted by gravity flow using elution buffer pH 7.5 (50 mM $Na_xH_yPO_4$, 300 mM NaCl, 250 mM imidazole, 20% glycerol, 1 mM 2-mercaptoethanol and 1 mM PMSF). Pure HMO2 was quantitated using Coomassie blue stained SDS–PAGE gels using bovine serum albumin as standard as well as by Micro BCA Protein Assay Kit (Pierce). At least three independent preparations of HMO2 were used, indicating reproducibility of the preparations. HMO1 was obtained as described earlier (37).

Agarose gel retardation

One hundred nanograms of supercoiled or linear pGEM5 was incubated at 4°C with different concentrations of HMO2 in 10 µl reaction buffer (20 mM Tris pH 8.0, 0.1 M EDTA, 15 mM NaCl, 0.1 mM DTT and 0.01% BRIJ 58). Complexes were resolved using 1% TBE agarose gels using 0.5× TBE buffer (50 mM Tris borate, 1 mM EDTA) and visualized by ethidium bromide staining.

DNA supercoiling

Supercoiled pUC18 was nicked using Nt.BstNBI (New England Biolabs). One hundred nanograms of nicked DNA was incubated with varying concentration of HMO2, at room temperature for 1 h. Reactions were initiated using 1 µl of 80 U/µl of T4 DNA ligase (New England Biolabs) in presence of ligase buffer and incubated at room temperature for 1 h. Reactions were terminated using 1 µl stop buffer (5 mM EDTA, 1.1% glycerol and 0.2 mg/ml proteinase K final concentration) and incubated at 37°C for 1 h. Samples were loaded on 1% TBE agarose gels and electrophoresed for 14 h followed by staining with ethidium bromide. For determination of the direction of DNA supercoils produced by HMO2, electrophoresis was performed in the presence of 0.3 µg/ml chloroquine, using *Bacillus subtilis* HU as a control.

Electrophoretic mobility shift assay

All oligonucleotides used for preparation of DNA constructs were purchased and purified by denaturing gel electrophoresis. Sequences are available in Supplementary Table S1. Electrophoretic Mobility Shift Assays (EMSAs) were performed using DNA duplex and DNA with loops, nicks, gaps and overhangs. A common 37-nt oligonucleotide was used to generate the different constructs. The top strand was 5′-end labeled using T4 polynucleotide kinase (New England Biolabs) and [γ^{32}P] ATP. The sequences of duplex as well as DNA with nick, gap, loops and overhangs were as described in (39) or presented in Supplementary Table S1. Top and bottom strands were annealed by heating at 90°C and slowly cooling to room temperature. Similarly, a 50 bp DNA duplex and duplex with either a single or tandem loops was generated by extending the 37 bp construct at both ends. Reactions contained 5 fmol of DNA substrate and varying concentration of HMO2 in 10 µl reaction buffer (20 mM Tris pH 8.0, 0.1 mM EDTA, 5 mM NaCl, 0.1 mM DTT, 0.01% BRIJ 58 and 0.1% Triton X-100) and incubated at room temperature for 1 h. Experiments designed to compare different DNA constructs were performed side-by-side with the same protein preparation. Samples were loaded on a prerun 8% polyacrylamide gel (39 : 1 acrylamide:bisacrylamide) and electrophoresed using 0.5× TBE at 175 V for 2 h.

Complexes were visualized using Amersham Biosciences Storm Phosphorimager. Reactions were performed at least in duplicate.

EMSA with four-way junctions

The sequence of the four-way junctions (4WJ) was described in (39) and shown in Supplementary Table S1. 4WJ were obtained by 5′-end labeling one strand and annealing the other three strands, followed by purification using native polyacrylamide gels. Complete annealing of all strands was determined by comparing the electrophoretic mobility to that of annealed constructs lacking one of the unlabeled strands. EMSA was performed as described above using 5 fmol of DNA and varying concentration of HMO2 in reaction buffer. Final volume of the reaction was 10 µl.

Competition assay

Five fmol 50-bp duplex DNA with loops and 4-µM of HMO2 was incubated at room temperature for 1 h in reaction buffer. Supercoiled or linear pGEM5 (0.5–50 fmol) was added and incubated at room temperature for 1 h; pGEM5 was linearized with NdeI or AatII. Samples were electrophoresed on prerun 8% polyacrylamide gels. Complexes were viewed using Storm Phosphorimager.

End-joining assay

Supercoiled pGEM5 was digested with NdeI or NaeI to obtain DNA with a 2-nt 5′ overhang or blunt ends, respectively. One hundred nanograms of linearized pGEM5 was incubated with varying concentrations of HMO2 or HMO1 at room temperature for 1 h. To this reaction, 1 µl of 400 U/µl of T4 DNA ligase was added and incubated at room temperature for 1 h. Samples were treated with exonuclease III (100 U/µl) at room temperature for 1 h. Reactions were terminated by adding 2 µl stop buffer (5 mM EDTA, 1.1% glycerol and 0.2 mg/ml proteinase K). Alternatively, supercoiled pET5a was digested with BspHI, which creates a 4-nt 5′ overhang. One hundred nanograms of the linearized pET5a was incubated with 2 µM HMO2. To this reaction 1 µl of 400 U/µl of T4 DNA ligase was added and incubated at room temperature for 1 h. Reactions were terminated by adding 2 µl of stop buffer. Samples were electrophoresed on 1% TBE agarose gels and visualized by ethidium bromide staining.

Using forward primer 5′-TGGGGTGCGAATTCTAA TGAGT-3′ and reverse primer 5′-GGCTTTACACTTTA TGCTTCCG-3′, an extra EcoRI site was introduced into plasmid pUC18 by PCR amplification. The pUC18 variant was then digested with EcoRI to obtain 105 bp DNA duplex with 5′-AATT extensions. The 105 bp DNA was 5′-end labeled using T4 polynucleotide kinase (New England Biolabs). One hundred femtomoles of 105 bp DNA was incubated with varying concentrations of HMO2 or 100 nM *B. subtilis* HU at room temperature for 1 h. To this reaction, 1 µl of 8 U/µl T4 DNA ligase was added and incubated at room temperature for 1 h. Samples were treated with exonuclease III (100 U/µl) at room temperature for 1 h. Reactions were terminated by adding 2 µl stop buffer and 1 µl of 10% SDS and then phenol chloroform extracted and ethanol precipitated. Samples were loaded on a prerun 5% polyacrylamide gel (39:1 acrylamide:bisacrylamide) and electrophoresed using 0.5× TBE at 175 V for 2 h. Complexes were visualized using Amersham Biosciences Storm Phosphorimager.

Exonuclease III protection assay

Supercoiled pGEM5 was linearized with NdeI or NaeI to yield DNA with 2-nt 5′ overhangs or blunt ends, respectively. pET5a was digested with BspHI to produce 4-nt 5′ overhang, pUC18 was digested with EcoRI, which also produces a 4-nt 5′ overhang, and a pcDNA3-derivative was digested with ApoI, which likewise creates a 4-nt 5′ overhang. pET5a was digested with ScaI and then PvuI (which cuts supercoiled DNA only poorly), to yield a blunt end and 2-nt 3′ overhang, respectively. pRAD1 was digested with DraI to produce blunt ends. Fifty to one hundred nanograms of linearized pGEM5, pET5a, pUC18, pcDNA3-derivative and pRAD1 was incubated at room temperature for 1 h with 2 µM HMO2 or HMO1 previously dialyzed using dialysis buffer (50 mM Tris pH 8.0, 50 mM NaCl and 20% glycerol). To each reaction, 1 µl of 100 U/µl exonuclease III was added and incubated at room temperature for 1 h. Reactions were terminated by addition of 2 µl 10% SDS or by phenol-extraction and ethanol precipitation (the latter in cases where shorter DNA fragments are produced that may co-migrate with SDS on the gels). Samples were electrophoresed on 1% TBE agarose gels. Gels were stained with ethidium bromide. All reactions were performed at least in duplicate, and pGEM5 digested with NdeI to produce 5′-TA overhangs was included for comparison to other DNA constructs.

DNase I protection assay

One hundred nanograms of supercoiled or linearized pGEM5 with blunt ends or overhangs were incubated at room temperature for 1 h with 1 µM HMO2 in 10 µl reaction buffer. One microliter of 0.1 U/µl DNaseI (New England Biolabs) was added in presence of DNase I buffer and incubated for 1, 2.5 and 5 min. Reactions were terminated by adding 2 µl of stop buffer and incubating at 37°C for 30 min, followed by addition of 1 µl of 10% SDS. Samples were electrophoresed on 1% TBE agarose gels. Gels were stained with ethidium bromide.

RESULTS

HMO2 binds preferentially to distorted DNA compared to linear duplex

While HMO2 has been proposed to interact with a damage-induced histone H2A variant, conservation of its Box B HMG-domain predicts direct DNA interaction. To investigate a potential role in DNA interaction, HMO2 was therefore cloned from yeast genomic DNA and overexpressed in *E. coli*. HMO2 was judged to be >95% pure using Coomassie blue stained SDS–PAGE gels

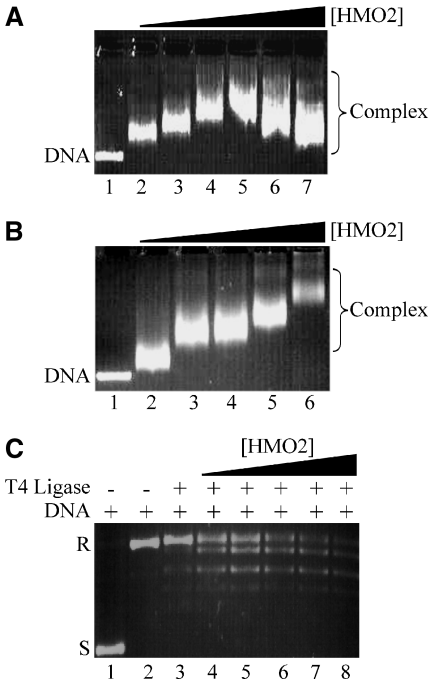

Figure 1. Interaction of HMO2 with plasmid DNA. (**A**, **B**) Agarose gel retardation of 100 ng plasmid DNA titrated with HMO2. (A) Reactions with supercoiled pGEM5. Lane 1, DNA only, lanes 2–7 with 1.0–6.0 μM HMO2. (B) Reactions with linearized pGEM5. Lane 1, DNA only, lanes 2–6 with 1.0–5.0 μM HMO2. (**C**) HMO2 supercoils relaxed DNA. Lane 1, 100 ng supercoiled pUC18 DNA. Lane 2, nicked pUC18. Lane 3, nicked pUC18 and T4 DNA ligase. Lanes 4–8, nicked DNA and T4 DNA ligase with 100, 500, 1000, 2000 and 3000 nM HMO2.

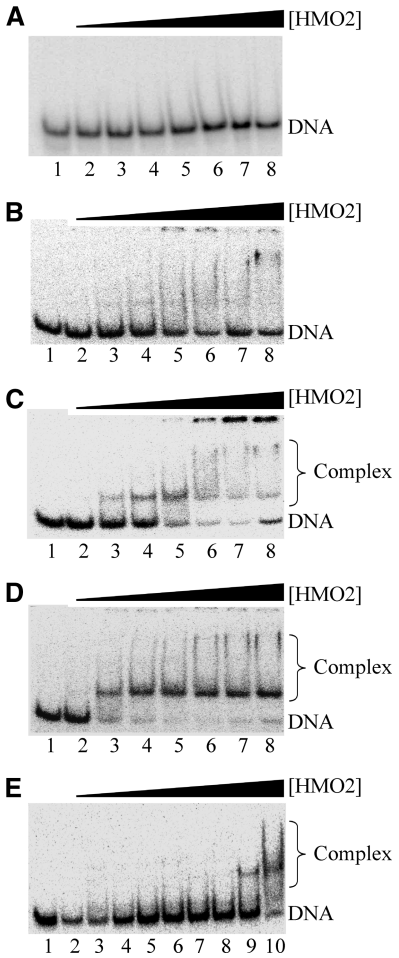

Figure 2. HMO2 binds preferentially to DNA with pairs of tandem mismatches. (**A**) EMSA of 50 bp DNA duplex and increasing concentrations of HMO2. (**B**, **C**) EMSA of 50 bp DNA duplex with a single loop (tandem mismatches) and increasing concentrations of HMO2; (B) loop composed of opposing AA nucleotides, (C) loop composed of opposing CT nucleotides. (**D**) EMSA of 50 bp DNA duplex with both AA and CT loops separated by 9 bp of duplex and increasing concentrations of HMO2. Lanes 1, reactions with DNA only, lanes 2–8, reactions with 50, 100, 500, 1000, 2000, 3000 and 4000 nM HMO2. (**E**) EMSA of four way junction DNA. Lane 1, 5 fmol of four way junction only. Lanes 2–10, reactions with 50, 100, 500, 1000, 2000, 3000, 4000, 5000 and 6000 nM HMO2.

(Supplementary Figure S1). Consistent with the presence of the classical Box B HMG domain, HMO2 binds both supercoiled and linear DNA (Figure 1) suggesting non-sequence-specific binding as seen for other chromatin-associated HMGB proteins. While the mobility of HMO2-associated linear DNA is gradually reduced as a function of [HMO2] (Figure 1B), the mobility of supercoiled DNA is enhanced at the highest [HMO2] (Figure 1A), suggesting DNA compaction. Note also that ethidium bromide staining of HMO2-bound DNA is enhanced compared to free DNA, perhaps reflecting a DNA unwinding by HMO2 that promotes dye-binding.

Like other HMGB proteins, HMO2 can constrain DNA supercoils (Figure 1C). When nicked plasmid was incubated with HMO2 in presence of T4 DNA ligase, HMO2 was found to introduce supercoils to the relaxed DNA. Electrophoresis in the presence of chloroquine indicates the expected introduction of negative supercoils by HMO2 (i.e., a slower migration of topoisomers in the presence of chloroquine; data not shown). This is in consensus with other HMGB proteins which can supercoil relaxed DNA (31). The ability of HMO2 to introduce supercoils is consistent with the DNA compaction seen on interaction with plasmid DNA (Figure 1A).

DNA binding was analyzed further using EMSA. HMO2 does not form detectable complex with 50-bp DNA duplex (Figure 2A) most likely reflecting that complexes are unstable and dissociate during electrophoresis since association with longer DNA clearly leads to stable complex formation (Figure 1). Mammalian HMGB was previously shown to bind preferentially to 37 bp DNA containing a pair of loops (tandem mismatches) separated by 9 bp of duplex (40). Using the same set of mismatches in the context of 50 bp duplex (Supplementary Table S1), HMO2 was seen to form a single stable complex (Figure 2D) indicating preferred binding to the looped DNA construct. Notably, association with the tandem-loop construct leads to enhanced complex formation compared to 50 bp DNA with a single loop (Figure 2B and C), and binding to the 50 bp duplex containing the CT loop (in which the sequence of the bottom strand contains a 3′-CT-5′-sequence, resulting in identical opposing bases; Figure 2C) is more stable than the 50 bp duplex with AA loop (Figure 2B), perhaps indicating that the sequence of the nucleotides at the loop results in differential DNA distortion, which in turn affects HMO2 binding

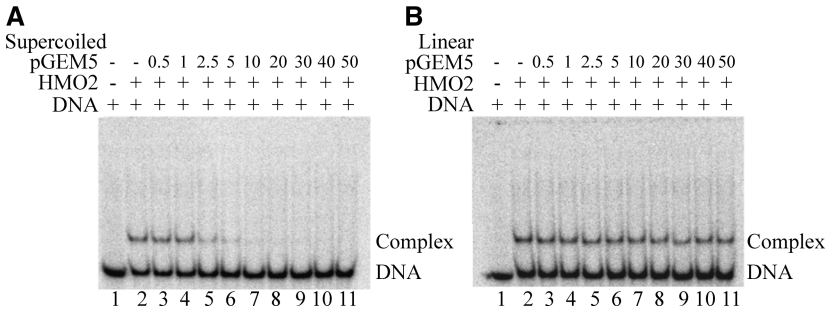

Figure 3. HMO2 binds preferentially to supercoiled DNA compared to linear DNA. (**A**) Reactions with 5 fmol of 50 bp looped DNA and 4 μM HMO2. Lane 1, DNA only, lanes 2, 50 bp looped DNA and 4 μM HMO2. Lanes 3–11 with 0.5–50 fmol supercoiled pGEM5. (**B**) Titration with linear pGEM5 with 5′ overhangs.

[an interpretation based on reported differential dynamic properties of DNA with different base mismatches; e.g., ref. (41)], or inherent sequence preferences of HMO2. Complex formation was generally more defined in presence of detergent as HMO2 self-associates in its absence (not shown); we therefore also had to consider the possibility that equilibrium binding conditions include a contribution from monomeric HMO2 dissociating from a larger aggregate when diluted from a concentrated stock solution, even in the presence of detergent, and we elected not to calculate a binding constant. Such self-association was also noted for the yeast HMGB homolog HMO1 (31,37,38). With the 37 bp DNA duplex with tandem loops, HMO2 forms an unstable but detectable complex, while no preferred binding was seen to 37 bp DNA with a single nick, gap or overhang (consistent with the observation that HMO2 binds preferentially to 50 bp DNA with two separate lesions; data not shown). In contrast to HMO1, HMO2 also does not form a detectable complex with 26 bp DNA (37). Evidently, HMO2 binds preferentially to DNA with a pair of lesions, but only in duplex DNA of sufficient length. On removal of the N-terminal His_6-tag, no difference was observed in DNA binding indicating that the presence of the His_6-tag does not interfere with DNA binding (data not shown).

HMGB proteins generally also have higher affinity for four-way junction DNA compared to perfect duplex DNA, provided the absence of Mg^{2+}, which would induce a disfavored stacked X conformation of the junctions (42–44). HMO2, however, has only a modest preference for the four-way DNA junctions in absence of Mg^{2+} (Figure 2E) compared to perfect duplex DNA and forms complex comparable to that seen with DNA containing a single lesion.

To ascertain whether HMO2 binds preferentially to supercoiled DNA, a competition assay was performed by incubating 5 fmol 50 bp looped DNA and 4 μM HMO2, following which 0.5–50 fmol of supercoiled or linearized pGEM5 was added to the reaction. Evidently, supercoiled DNA competes more efficiently (Figure 3); HMO2 forms a distinct complex with the looped DNA while supercoiled DNA competes as indicated by disappearance of the preformed complex. The linearized DNA does not compete at equivalent concentrations whether the DNA has 5′ overhangs, 3′ overhangs or blunt ends (Figure 3B and data not shown; note that the concentration of free DNA ends is at most 10 nM, well below the concentration of HMO2, while the concentration of internal sites would be more than two orders-of-magnitude higher, assuming a 20 bp site size). This suggests that HMO2 binds to supercoiled DNA with higher affinity compared to linearized DNA. Taken together, our data indicate that HMO2 resembles mammalian HMGB proteins in its preferred binding to supercoiled DNA or DNA with tandem mismatches, but that it distinguishes itself by its requirement for a longer DNA duplex and its preference for DNA with a pair of lesions.

HMO2 binds DNA ends

HMGB proteins have been reported to promote DNA end-joining *in vitro* (26,27). The *in vivo* correlate would be that during DSB repair, HMGB might bring two DNA ends in closer proximity in preparation for either HR or NHEJ. HMO2, however, did not promote the formation of end-joined products in the presence of T4 DNA ligase. Instead, HMO2 prevented end-joining of DNA with a 5′-TA extension (Figure 4A) or DNA with blunt ends (Figure 4B). In Figure 4A and B, lane 2 shows 100 ng (~4 nM) linearized DNA ligated in presence of T4 DNA ligase. But in presence of HMO2 (0.1–4 μM; lanes 3–8) there are few if any end-joined products. By comparison, 100 ng plasmid DNA (~2 nM) may be efficiently ligated in the presence of mammalian HMGB1, with optimal ligation efficiency seen on addition of ~1 μM HMGB1 (26). Notably, lane 9 suggests that the DNA is resistant to exonuclease III digestion in the presence of HMO2 and T4 DNA ligase. The failure to observe ligation products in presence of HMO2 as well as the inability of exonuclease III to digest the DNA suggests that HMO2 may be binding to the ends of the DNA duplex to prevent access to both T4 DNA ligase and exonuclease III. Also note that failure to join DNA ends is not due to HMO2 merely interacting with the ligase to prevent its activity, as evidenced by the activity of T4 DNA ligase on an internal DNA nick in the presence of HMO2 (Figure 1C).

To examine further a potential DNA end-binding by HMO2, DNA with a 2-nt 5′-TA extension or blunt ends (Figure 5A) and DNA with a 2-nt 3′-AT extension

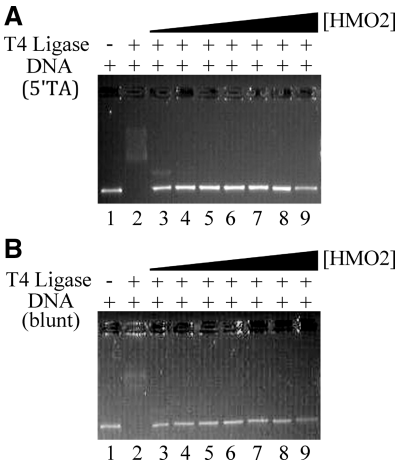

Figure 4. HMO2 prevents ligation of DNA by T4 DNA ligase. (**A**) DNA with overhangs (5′-TA extensions). (**B**) DNA with blunt ends. Lanes 1, 100 ng of DNA (~4 nM, corresponding to ~8 nM DNA ends). Lane 2, DNA and T4 DNA ligase. Lanes 3–8, DNA, T4 DNA ligase with 100, 500, 1000, 2000, 3000 and 4000 nM HMO2. Lane 9, DNA, T4 DNA ligase, 4000 nM HMO2 and exonuclease III.

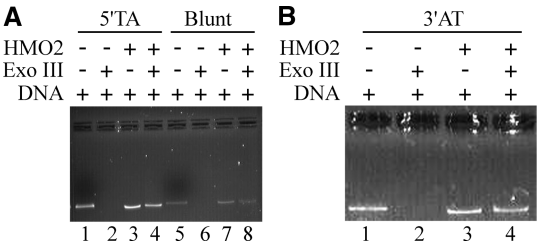

Figure 5. HMO2 protects DNA with overhangs or blunt ends from exonucleolytic cleavage. (**A**) Lanes 1–4 and 5–8, DNA with 2-nt 5′-TA extensions (~4 nM) and blunt ends (~2 nM), respectively. Lanes 1 and 5, DNA only. Lanes 3 and 7, DNA and 2000 nM HMO2. Lanes 2 and 6, DNA treated with exonuclease III for 1 h. Lanes 4 and 8, DNA with 1000 nM HMO2 incubated with exonuclease III for 1 h. (**B**) DNA with 2-nt 3′-AT extensions (~4 nM). Lane 1, DNA only. Lane 2, DNA treated with exonuclease III for 1 h. Lane 3, DNA with 2-nt 3′ overhangs and 2000 nM HMO2. Lane 4, DNA incubated with HMO2 and exonuclease III for 1 h.

(Figure 5B) was treated with exonuclease III in presence of HMO2. Exonuclease III reactions are terminated with SDS, and a control in which HMO2 is incubated with DNA in absence of exonuclease III is included (lane 3); in the latter reactions, the original DNA is quantitatively recovered upon treatment with SDS, indicating complete disruption of the HMO2–DNA complex, which would otherwise be manifest as a mobility shift as seen in Figure 1. Figure 5A, lanes 2 and 6 and Figure 5B, lane 2, shows DNA with 5′ overhangs, blunt ends and 3′ overhangs digested extensively by exonuclease III. But in presence of HMO2, the DNA is protected (Figure 5A, lanes 4 and 8; B, lane 4). Since HMO2 obviously prevents the formation of partial digestion products, as it prevents the more extensive digestion seen on prolonged incubation with exonuclease III, we elected to show only the time-point at which exonuclease III has digested unprotected DNA to such an extent that no individual bands are discernible. These data suggest that HMO2 may be binding to both DNA with 5′ and 3′ overhangs or blunt ends and preventing exonuclease III from accessing the ends.

If HMO2 binds stably to DNA ends, preventing access of both T4 DNA ligase and exonuclease III, then the expectation would have been for stable complex formation with 50 bp DNA duplex. This is not observed (Figure 2A). Furthermore, we do not observe protection of 50 bp DNA from exonuclease III-digestion in the presence of HMO2 (data not shown). We therefore considered that the 50 bp DNA might be too short to accommodate HMO2 stably at both ends simultaneously. To address this question, plasmid DNA was digested with assorted enzymes to yield fragments of different sizes. When plasmid pET5a is digested with BspHI, four fragments are produced that contain 5′-CATG extensions. However, when incubated with HMO2 and exonuclease III, no protection is observed (Figure 6A, lane 4), while DNA with 5′-TA extension is protected from exonucleolytic digestion (lane 8). Consistent with the inability of HMO2 to protect DNA with BspHI-generated 5′ overhangs, such DNA may be re-ligated in presence of T4 DNA ligase (Figure 6B, lane 3; lanes 1 and 2 contain DNA without and with T4 DNA ligase, respectively). That ligation products obtained in the presence of HMO2 migrate differently compared to those created in its absence may suggest either that HMO2 still binds with sufficient affinity to the 5′-CATG overhangs to compete with ligase for binding or that binding to internal sites results in a DNA conformation that favors formation of a different population of ligation products. Since DNA with 5′-AATT extensions is efficiently protected (Figure 6C), our data suggest that it is the sequence of the overhangs that affects HMO2 binding. The differential protection of DNA of comparable length, but with distinct sequence of the single-stranded overhang, clearly indicates that HMO2 recognizes specific features of DNA ends.

To determine the DNA length required for efficient protection by HMO2, we therefore used enzymes that produce blunt ends or A + T-containing overhangs. A pCDNA3-derivative when linearized with ApoI produces the following sizes of DNA, 127, 187, 811, 848, 1444, 1475 and 2277 bp. Figure 6C, lane 4 shows that HMO2 could efficiently protect 811, 848, 1444, 1475 and 2277 bp but was unable to protect 127 and 187 bp DNA, indicating that a suitable size of the DNA is important for HMO2 in order to protect it from exonucleolytic cleavage. Consistent with this observation, HMO2 was able to protect 339, 692 and 713 bp fragments of pRAD1 linearized with DraI (data not shown). This suggests that not only the size of the DNA but also the sequence of the DNA overhang is important for HMO2 to bind and protect the DNA.

The failure to protect short DNA from exonuclease III digestion, even if single-stranded overhangs are otherwise compatible with HMO2-binding, predicts that such duplexes should be ligatable in presence of HMO2. We therefore performed an end-joining assay using 105 bp DNA with 5′-AATT overhangs. Figure 6D shows that

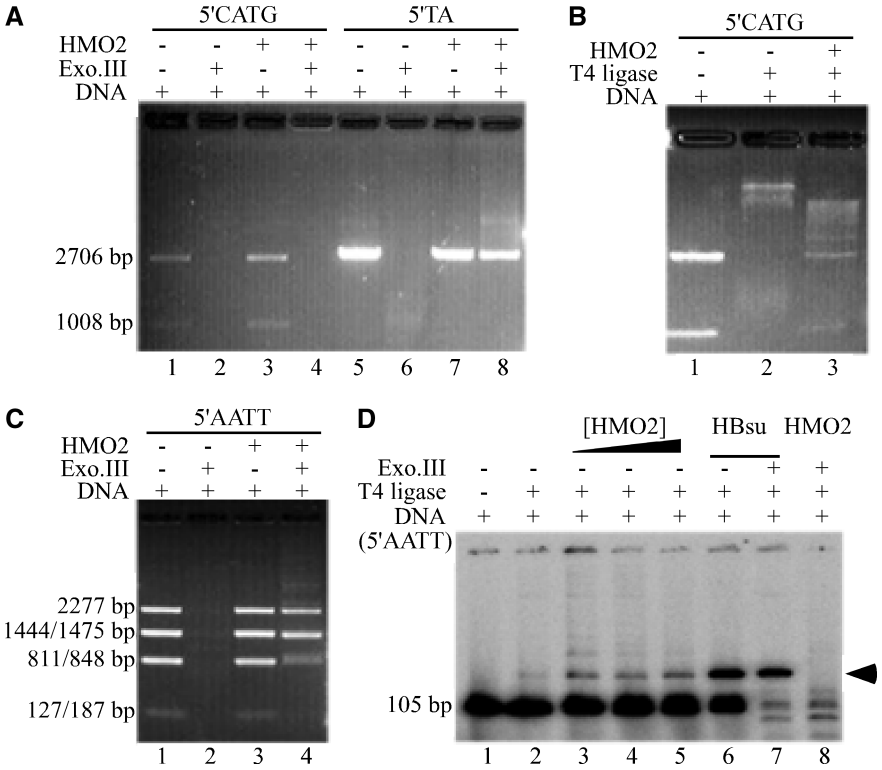

Figure 6. DNA protection by HMO2 depends on DNA length and sequence of DNA overhangs. (**A**) DNA with G + C-containing overhangs is not protected by HMO2. Lanes 1–4, DNA with 5′-CATG extensions (~2 nM), lanes 5–8, DNA with 5′-TA extensions (~4 nM). Lanes 1 and 5, DNA only. Lanes 2 and 6, DNA treated with exonuclease III for 1 h. Lanes 3 and 7, DNA and 2000 nM HMO2. Lanes 4 and 8, DNA with 2000 nM HMO2 incubated with exonuclease III for 1 h. Note in lane 8 the appearance of a product with lower mobility. Only the two largest fragments of BspHI-digested pET5a are shown in lanes 1–4. (**B**) Ligation of DNA with 5′-CATG extension (~2 nM). Lane 1, DNA only. Lane 2, DNA and T4 DNA ligase. Lane 3, DNA, T4 DNA ligase and 2.5 μM HMO2. (**C**) Length dependence of DNA protection by HMO2. Lane 1, DNA with 4-nt 5′ overhangs. Lane 2, DNA treated with exonuclease III for 1 h. Lane 3, DNA and 2000 nM HMO2. Lane 4, DNA incubated with HMO2 and exonuclease III for 1 h. (**D**) HMO2 can end-join 105 bp DNA in presence of T4 DNA ligase. Lane 1, 100 fmol of 105 bp DNA. Lane 2, 105 bp DNA and T4 DNA ligase. Lanes 3–5, 105 bp DNA, T4 DNA ligase and 100, 250 and 500 nM HMO2. Lane 6, 105 bp DNA, T4 DNA ligase and 100 nM *B. subtilis* HU (HBsu). Lane 7, 105 bp DNA, T4 DNA ligase, 100 nM *B. subtilis* HU and exonuclease III. Lane 8, 105 bp DNA, T4 DNA ligase, 250 nM HMO2 and exonuclease III.

HMO2 promotes DNA dimer formation in presence of T4 DNA ligase (lanes 3–5). Similar reactions with *B. subtilis* HU indicate formation of monomer circle, as evidenced by its protection from exonuclease III digestion (lanes 6 and 7). Lane 8 indicates that ligation products with 105 bp obtained in presence of HMO2 cannot be protected from exonuclease III. This experiment not only confirms the inability of HMO2 to associate with the ends of short DNA in a manner that prevents access to ligase and exonuclease III, but it also reveals that HMO2 does not promote cyclization of short DNA. Whether this reflects an inability of HMO2 to bend DNA, the association of several HMO2 protomers causing out-of-phase bending, or preferred binding to DNA ends remains to be determined.

To rule out the possibility that HMO2 may coat or compact the entire DNA, thereby rendering the majority of the DNA resistant to exonuclease digestion, we assessed whether HMO2–DNA complexes are also resistant to endonucleolytic digestion. Supercoiled DNA or linear DNA with overhangs or blunt ends were treated with DNase I. Figure 7, lanes 2, 8 and 14 show DNA treated with DNaseI wherein the DNA is digested extensively.

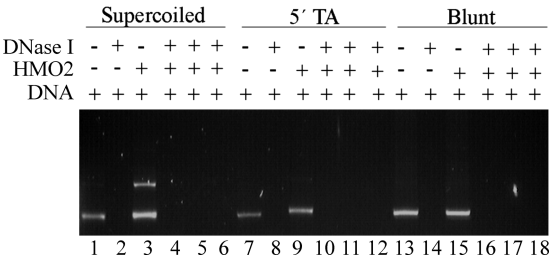

Figure 7. HMO2 does not protect supercoiled or linearized DNA from endonucleolytic cleavage. Lanes 1–6, 7–12 and 13–18, supercoiled DNA, DNA with overhangs and DNA with blunt ends, respectively (~4 nM). Lanes 1, 7 and 13, DNA only. Lanes 3, 9 and 15, DNA and 1000 nM HMO2. Lanes 2, 8 and 14, DNA treated with DNase I for 2.5 min. Lanes 4, 5 and 6, supercoiled DNA and 1000 nM HMO2 treated with DNase I for 1, 2.5 and 5 min. Lanes 10, 11 and 12, DNA with overhangs and 1000 nM HMO2 treated with DNase I for 1, 2.5 and 5 min. Lanes 16, 17 and 18, DNA with blunt ends and 1000 nM HMO2 treated with DNase I for 1, 2.5 and 5 min.

In presence of HMO2, DNaseI is likewise able to digest the DNA (lanes 4–6, 10–12 and 16–18). The inability of HMO2 to attenuate endonucleolytic digestion is consistent with the interpretation that protection against

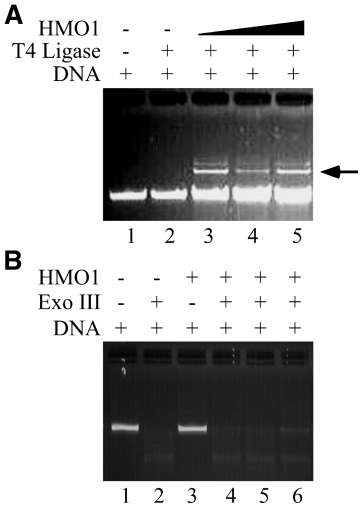

Figure 8. HMO1 promotes DNA end-joining, but does not protect DNA from exonucleolytic cleavage. (**A**) HMO1 can promote end-joining of pGEM5 DNA with 2-nt 5′ overhang in presence of T4 DNA ligase. Lane 1, 100 ng DNA only. Lane 2, DNA and T4 DNA ligase. Lanes 3–5, DNA, T4 DNA ligase, and 500, 1000 and 2000 nM HMO1, respectively. (**B**) HMO1 is unable to protect DNA with 2-nt 5′ overhangs from exonuclease III. Lane 1, 100 ng DNA only. Lane 2, DNA and exonuclease III. Lane 3, DNA and 500 nM HMO1. Lanes 4–6, DNA, exonuclease III, and 500, 1000 and 2000 nM HMO1, respectively.

exonuclease III-mediated digestion is due to end-binding by HMO2, not continuous protection of internal sites.

To document further that the very stable binding to DNA ends that is characteristic of HMO2 is unique and not a general property of the yeast HMGB proteins, we performed the equivalent assays with HMO1. As shown in Figure 8, properties of HMO1 are more akin to those of mammalian HMGB1; it does promote the association of DNA ends in the presence of DNA ligase (Figure 8A), but it either does not bind to DNA ends or does so only transiently to allow efficient access to exonuclease III, as evidenced by its failure to protect linearized pGEM5 with 2-nt 5′ overhangs from exonucleolytic cleavage (Figure 8B, lanes 4–6).

DISCUSSION

Preferential binding to distorted DNA

The occluded DNA site size for an HMG domain is ~10 bp (19–23). Since HMO2 has two domains, Box A and Box B, it would be predicted to require at least a 20 bp DNA site; indeed, the yeast HMGB homolog HMO1, which also features two HMG-like domains, binds poorly to 18 bp DNA, but with significantly higher affinity to 26 bp DNA (37). However, our data suggest that HMO2 binds only weakly to 37 bp DNA with loops (data not shown) and with much greater affinity to 50 bp looped DNA (Figure 2). For the Box B domain, which has high homology to mammalian HMGB proteins, interaction with a 10 bp site is a strong prediction. Although the Box A domain differs from consensus HMG sequences, its similarity to the HMO1 Box A domain, which also differs from consensus sequences, yet interacts with an ~10 bp site, likewise predicts an ~10 bp site. Based on these assumptions about the site sizes for Box A and Box B, a 50 bp DNA construct would be of sufficient length to accommodate a dimer; this interpretation does not necessarily imply that HMO2 likewise binds perfect duplex DNA as a dimer, as the loops may potentially impose a constraint, such as preferred binding to the 4-nt loop by only one of the two protein domains.

HMGB proteins have been previously shown to bind DNA with loops (40,45). The binding preference for DNA with flexure points is a functional correlate of the DNA bend introduced on interaction with an HMG domain, and the prediction is that HMO2 likewise bends its DNA site. HMGB proteins also bind preferably to four-way DNA junctions (42–44); while HMO2 does bind four-way DNA junctions in preference to a linear DNA duplex (compare Figure 2A and E), the preference is modest. For mammalian HMGB1, binding to four-way DNA junctions is mediated by the Box A domain (44). This selectivity arises from using a hydrophobic residue from helix II of the HMG fold as a bending wedge; the greater preference for distorted DNA is due to stacking of this residue on an exposed base pair. In contrast, mammalian HMGB1 Box B has bending wedges in both helices I and II of the HMG fold and is primarily responsible for DNA bending, whereas its affinity for distorted DNA is only modestly higher than that for perfect duplex DNA. By comparison, HMO2 is also predicted to feature a bending wedge (Leu) in helix II of its Box A domain, suggesting that this domain contributes the binding preference for distorted DNA. For HMO2 Box B, a leucine in helix I would be predicted to be the DNA intercalating residue.

Like other HMGB proteins, HMO2 binds preferentially to supercoiled DNA compared to linear DNA (Figures 1 and 3). The DNA–protein complex with highest [HMO2] migrates faster in the gel (Figure 1, lanes 6 and 7), suggesting that HMO2 might play a role in DNA compaction. This observation is consistent with the ability of HMO2 to introduce supercoils and with the enhanced staining of HMO2-bound DNA by ethidium bromide that may also reflect DNA unwinding by HMO2. While nuclear HMGB proteins have not been shown to compact DNA *in vitro* as determined by changes in electrophoretic mobility, Abf2p, a protein closely related to the HMG family, has been shown to compact mitochondrial DNA (46). Long-range DNA looping created by protein–protein contacts, however, has been shown to produce more compact DNA structures (47).

DNA-end binding

Consistent with its preferred binding to negatively supercoiled DNA, HMO2 produces DNA supercoils, due either to DNA underwinding or out-of-plane bending. And as noted above, its preferred binding to DNA loops likely reflects the energetic advantage to bending DNA with flexible joints. In these interactions, HMO2 emulates properties of mammalian HMGB homologs. What is unique about HMO2 is its remarkable ability to protect certain DNA constructs from exonucleolytic cleavage and

to prevent their end-joining in presence of T4 DNA ligase, suggesting preferred binding to these DNA ends. DNA with blunt ends is protected efficiently, while in case of DNA with overhangs, the sequence of the single stranded overhang significantly affects HMO2 binding (Figures 5A, B, and 6A). Considering the preferred binding of HMO2 to distorted DNA sites, its interaction with DNA ends may likewise be a manifestation of preferred binding to more deformable duplex regions. Mammalian HMGB1 has been reported to bind DNA ends, but not to protect DNA ends from exonuclease III, perhaps reflecting a more dynamic association with the DNA ends (26). The ability of HMO2 to associate more stably with DNA ends is perhaps attributable to the divergent Box A domain which bears little resemblance to mammalian Box A.

It is also evident that HMO2 requires DNA of a suitable length to bind and protect (Figure 6C). Since HMO2 forms stable complex with plasmid DNA, but not with 50 bp perfect duplex, and since it appears to bind only as a dimer to 50 bp looped DNA, complex stability is likely a consequence of both DNA structure and protein–protein interactions. Such interactions are likely the reason for protection only of DNA long enough for assembly of several protomers at each DNA end. Self-association was also reported for the yeast HMGB homolog HMO1 as well as for mammalian HMGB1, for which residues in the box B domain critical for its ability to stimulate DNA end-joining were also important for box B self-association on supercoiled DNA and the formation of large nucleoprotein complexes (26,31,37).

If HMO2 were to protect DNA from exonuclease III digestion largely by occluding essentially the entire DNA, except for a limited number of base pairs at the ends, then protection from endonuclease digestion might also be seen. However, no such protection is observed (Figure 7). For this interpretation to be considered, one would also expect that all DNA fragments, regardless of sequence of the DNA overhangs, would be protected comparably. This is also not observed, as evidenced by the failure of HMO2 to protect DNA with C- or G-containing overhangs (Figure 6A and B). We also note that ligation at an internal nick occurs in the presence of HMO2 (Figure 1C). For HMO2 to bend internal sites, thereby restricting access to exonuclease III and DNA ligase is likewise unlikely; first, attenuated access to endonuclease would again be expected, as would protection of DNA fragments regardless of sequence of DNA overhangs. If significant out-of-phase bending occurred upon HMO2 binding, this could stiffen DNA and prevent net DNA bending, resulting in preferential generation of linear ligation products in preference to circular products, an effect likely to be most pronounced using shorter DNA fragments as opposed to plasmid DNA. Indeed, facilitated cyclization of short DNA fragments in presence of a DNA-bending protein is commonly used as an assay for DNA bending, without internal DNA bends restricting access of DNA ligase to DNA ends (27,37). In-phase bending might lead to compaction; such compacted DNA may be produced by both HMGB homologs and the bacterial histone-like HU proteins, again without restricting access of DNA ends to DNA ligase (48). Based on these observations and considerations, we therefore conclude that HMO2 exerts its protection against exonuclease III by binding to the DNA ends.

If DNA with complementary overhangs were to anneal, a duplex with nicks would be produced. However, it can also be ruled out that HMO2 merely binds preferentially to such nicked DNA constructs to prevent their ligation, as short DNA with equivalent overhangs may be ligated (Figure 6D). Nicked plasmid DNA may likewise be ligated in the presence of HMO2 (Figure 1C). Indeed, the enhanced ligation of 105 bp DNA in the presence of HMO2 suggests that HMO2 may also bind the ends of the shorter DNA, albeit less stably, as reflected in its inability to protect such duplexes from exonucleolytic digestion. That HMO2 promotes DNA end-joining in the presence of DNA ligase may also be related to the occasional appearance of more slowly migrating DNA species following incubation of linear DNA with both HMO2 and exonuclease III (Figure 6A, lane 8); since these reactions are deproteinized and no ligase is present, we surmise that long single-stranded overhangs generated by exonuclease may invade a complementary duplex in presence of HMO2 to generate a merged structure that is stable to the subsequent manipulations. This possibility is currently under investigation.

Recently, HMO2 was reported to be a part of the ATP-dependent chromatin-remodeling complex INO80 and to be important for recruitment of the INO80 complex to a DSB (3). Arrival of the INO80 complex is predicted to be a part of the early response to DSB formation. In both mammalian and yeast cells, a complex containing the Ku heterodimer and DNA ligase is capable of rejoining DNA DSBs with compatible ends via NHEJ, while DNA with damaged ends requires additional factors (2,4). Furthermore, NHEJ and HR events interfere with each other; for example, a Rad51 filament forms on single-stranded DNA in preparation for HR and impedes NHEJ (49). It is conceivable, therefore, that HMO2, in addition to its role in INO80 recruitment, also contributes to the protection of DNA ends that is essential to preserve the genetic information before DSB repair can be completed. In its complex with INO80 components, HMO2 was reported to interact with phosphorylated histone H2A, indicating that it is not buried in the complex, but accessible for interaction with chromatin. It is therefore likely that it would also be accessible for binding to naked DNA. The preferred binding to DNA with blunt ends or with A + T-containing overhangs may indicate differential functions depending on the type of DNA ends and the DNA repair pathway; for example, yeast Rad51 binds more slowly to single-stranded DNA with AT dinucleotide repeats compared to C- or G-containing dinucleotide repeats (50), perhaps requiring accessory proteins to protect such A + T-rich sequences.

SUPPLEMENTARY DATA

Supplementary Data are available at NAR Online.

ACKNOWLEDGMENTS

The authors thank Dr LiJuan Xiao for providing HMO1.

FUNDING

National Science Foundation [MCB-0414875 and MCB-0744240 to A.G.].

Conflict of interest statement. None declared.

REFERENCES

1. van Attikum,H. and Gasser,S.M. (2005) ATP-dependent chromatin remodeling and DNA double-strand break repair. *Cell Cycle*, **4**, 1011–1014.
2. Sonoda,E., Hochegger,H., Saberi,A., Taniguchi,Y. and Takeda,S. (2006) Differential usage of non-homologous end-joining and homologous recombination in double strand break repair. *DNA Repair*, **5**, 1021–1029.
3. Morrison,A.J., Highland,J., Krogan,N.J., Arbel-Eden,A., Greenblatt,J.F., Haber,J.E. and Shen,X. (2004) INO80 and gamma-H2AX interaction links ATP dependent chromatin remodeling to DNA damage repair. *Cell*, **119**, 767–775.
4. Paques,F. and Haber,J.E. (1999) Multiple pathways of recombination induced by double-strand breaks in *Saccharomyces cerevisiae*. *Microbiol. Mol. Biol. Rev*., **63**, 349–404.
5. Bird,A.W., Yu,D.Y., Pray-Grant,M.G., Qiu,Q., Harmon,K.E., Megee,P.C., Grant,P.A., Smith,M.M. and Christman,M.F. (2002) Acetylation of histone H4 by Esa1 is required for DNA double-strand break repair. *Nature*, **419**, 411–415.
6. Jazayeri,A., McAinsh,A.D. and Jackson,S.P. (2004) *Saccharomyces cerevisiae* Sin3p facilitates DNA double-strand break repair. *Proc. Natl Acad. Sci. USA*, **101**, 1644–1649.
7. Jin,J., Cai,Y., Yao,T., Gottschalk,A.J., Florens,L., Swanson,S.K., Gutierrez,J.L., Coleman,M.K., Workman,J.L., Mushegian,A. *et al*. (2005) A mammalian chromatin remodeling complex with similarities to the yeast INO80 complex. *J. Biol. Chem*., **280**, 41207–41212.
8. Shen,X., Mizuguchi,G., Hamiche,A. and Wu,C. (2000) A chromatin remodelling complex involved in transcription and DNA processing. *Nature*, **406**, 541–544.
9. Shen,X., Ranallo,R., Choi,E. and Wu,C. (2003) Involvement of actin-related proteins in ATP-dependent chromatin remodeling. *Mol. Cell*, **12**, 147–155.
10. van Attikum,H., Fritsch,O., Hohn,B. and Gasser,S.M. (2004) Recruitment of the INO80 complex by H2A phosphorylation links ATP-dependent chromatin remodeling with DNA double-strand break repair. *Cell*, **119**, 777–788.
11. van Attikum,H., Fritsch,O. and Gasser,S.M. (2007) Distinct roles for SWR1 and INO80 chromatin remodeling complexes at chromosomal double-strand breaks. *EMBO J*., **26**, 4113–4125.
12. Bustin,M. (1999) Regulation of DNA-dependent activities by the functional motifs of the high-mobility-group chromosomal proteins. *Mol. Cell Biol*., **19**, 5237–5246.
13. Bustin,M. (2001) Revised nomenclature for high mobility group (HMG) chromosomal proteins. *Trends. Biochem. Sci*., **26**, 152–153.
14. Wong,B., Masse,J.E., Yen,Y.M., Giannikopoulos,P., Feigon,J. and Johnson,R.C. (2002) Binding to cisplatin-modified DNA by the *Saccharomyces cerevisiae* HMGB protein Nhp6A. *Biochemistry*, **41**, 5404–5414.
15. Travis,A., Amsterdam,A., Belanger,C. and Grosschedl,R. (1991) LEF-1, a gene encoding a lymphoid-specific protein with an HMG domain, regulates T-cell receptor alpha enhancer function [corrected]. *Genes Dev*., **5**, 880–894.
16. Sinclair,A.H., Berta,P., Palmer,M.S., Hawkins,J.R., Griffiths,B.L., Smith,M.J., Foster,J.W., Frischauf,A.M., Lovell-Badge,R. and Goodfellow,P.N. (1990) A gene from the human sex-determining region encodes a protein with homology to a conserved DNA-binding motif. *Nature*, **346**, 240–244.
17. Love,J.J., Li,X., Case,D.A., Giese,K., Grosschedl,R. and Wright,P.E. (1995) Structural basis for DNA bending by the architectural transcription factor LEF-1. *Nature*, **376**, 791–795.
18. Moreira,J.M. and Holmberg,S. (2000) Chromatin-mediated transcriptional regulation by the yeast architectural factors NHP6A and NHP6B. *EMBO J*., **19**, 6804–6813.
19. Allain,F.H., Yen,Y.M., Masse,J.E., Schultze,P., Dieckmann,T., Johnson,R.C. and Feigon,J. (1999) Solution structure of the HMG protein NHP6A and its interaction with DNA reveals the structural determinants for non-sequence-specific binding. *EMBO J*., **18**, 2563–2579.
20. Stott,K., Tang,G.S., Lee,K.B. and Thomas,J.O. (2006) Structure of a complex of tandem HMG boxes and DNA. *J. Mol. Biol*., **360**, 90–104.
21. Klass,J., Murphy,F.V. 4th, Fouts,S., Serenil,M., Changela,A., Siple,J. and Churchill,M.E. (2003) The role of intercalating residues in chromosomal high-mobility-group protein DNA binding, bending and specificity. *Nucleic Acids Res*., **31**, 2852–2864.
22. Jung,Y. and Lippard,S.J. (2003) Nature of full-length HMGB1 binding to cisplatin-modified DNA. *Biochemistry*, **42**, 2664–2671.
23. Ohndorf,U.M., Rould,M.A., He,Q., Pabo,C.O. and Lippard,S.J. (1999) Basis for recognition of cisplatin-modified DNA by high-mobility-group proteins. *Nature*, **399**, 708–712.
24. Yamanaka,S., Katayama,E., Yoshioka,K., Nagaki,S., Yoshida,M. and Teraoka,H. (2002) Nucleosome linker proteins HMGB1 and histone H1 differentially enhance DNA ligation reactions. *Biochem. Biophys. Res. Commun*., **292**, 268–273.
25. Reeves,R. and Adair,J.E. (2005) Role of high mobility group (HMG) chromatin proteins in DNA repair. *DNA Repair*, **4**, 926–938.
26. Stros,M., Cherny,D. and Jovin,T.M. (2000) HMG1 protein stimulates DNA end joining by promoting association of DNA molecules via their ends. *Eur. J. Biochem*., **267**, 4088–4097.
27. Ugrinova,I., Mitkova,E., Moskalenko,C., Pashev,I. and Pasheva,E. (2007) DNA bending versus DNA end joining activity of HMGB1 protein is modulated in vitro by acetylation. *Biochemistry*, **46**, 2111–2117.
28. Kruppa,M., Moir,R.D., Kolodrubetz,D. and Willis,I.M. (2001) Nhp6, an HMG1 protein, functions in SNR6 transcription by RNA polymerase III in *S. cerevisiae*. *Mol. Cell*, **7**, 309–318 .
29. Lopez,S., Livingstone-Zatchej,M., Jourdain,S., Thoma,F., Sentenac,A. and Marsolier,M.C. (2001) High-mobility-group proteins NHP6A and NHP6B participate in activation of the RNA polymerase III SNR6 gene. *Mol. Cell Biol*., **21**, 3096–3104.
30. Kassavetis,G.A. and Steiner,D.F. (2006) Nhp6 is a transcriptional initiation fidelity factor for RNA polymerase III transcription *in vitro* and *in vivo*. *J. Biol. Chem*., **281**, 7445–7451.
31. Lu,J., Kobayashi,R. and Brill,S.J. (1996) Characterization of a high mobility group 1/2 homolog in yeast. *J. Biol. Chem*., **271**, 33678–33685.
32. Gadal,O., Labarre,S., Boschiero,C. and Thuriaux,P. (2002) Hmo1, an HMG-box protein, belongs to the yeast ribosomal DNA transcription system. *EMBO J*., **21**, 5498–5507.
33. Hall,D.B., Wade,J.T. and Struhl,K. (2006) An HMG protein, Hmo1, associates with promoters of many ribosomal protein genes and throughout the rRNA gene locus in *Saccharomyces cerevisiae*. *Mol. Cell Biol*., **26**, 3672–3679.
34. Berger,A.B., Decourty,L., Badis,G., Nehrbass,U., Jacquier,A. and Gadal,O. (2007) Hmo1 is required for TOR-dependent regulation of ribosomal protein gene transcription. *Mol. Cell Biol*., **27**, 8015–8026.
35. Merz,K., Hondele,M., Goetze,H., Gmelch,K., Stoeckl,U. and Griesenbeck,J. (2008) Actively transcribed rRNA genes in *S. cerevisiae* are organized in a specialized chromatin associated with the high-mobility group protein Hmo1 and are largely devoid of histone molecules. *Genes Dev*., **22**, 1190–1204.
36. Xiao,L. and Grove,A. (2009) Coordination of ribosomal protein and ribosomal RNA gene expression in response to TOR signaling. *Curr. Genomics*, **10**, 198–205.
37. Kamau,E., Bauerle,K.T. and Grove,A. (2004) The *Saccharomyces cerevisiae* high mobility group box protein HMO1 contains two functional DNA binding domains. *J. Biol. Chem*., **279**, 55234–55240.

38. Bauerle,K.T., Kamau,E. and Grove,A. (2006) Interactions between N- and C-terminal domains of the *Saccharomyces cerevisiae* high-mobility group protein HMO1 are required for DNA bending. *Biochemistry*, **45**, 3635–3645.
39. Ghosh,S. and Grove,A. (2004) Histone-like protein HU from *Deinococcus radiodurans* binds preferentially to four-way DNA junctions. *J. Mol. Biol.*, **337**, 561–571.
40. Grove,A., Galeone,A., Mayol,L. and Geiduschek,E.P. (1996) Localized DNA flexibility contributes to target site selection by DNA-bending proteins. *J. Mol. Biol.*, **260**, 120–125.
41. Patel,D.J., Kozlowski,S.A., Ikuta,S. and Itakura,K. (1984) Dynamics of DNA duplexes containing internal G.T, G.A, A.C, and T.C pairs: hydrogen exchange at and adjacent to mismatch sites. *Fed. Proc.*, **43**, 2663–2670.
42. Ferrari,S., Harley,V.R., Pontiggia,A., Goodfellow,P.N., Lovell-Badge,R. and Bianchi,M.E. (1992) SRY, like HMG1, recognizes sharp angles in DNA. *EMBO J.*, **11**, 4497–4506.
43. Pöhler,J.R., Norman,D.G., Bramham,J., Bianchi,M.E. and Lilley,D.M. (1998) HMG box proteins bind to four-way DNA junctions in their open conformation. *EMBO J.*, **17**, 817–826.
44. Webb,M. and Thomas,J.O. (1999) Structure-specific binding of the two tandem HMG boxes of HMG1 to four-way junction DNA is mediated by the A domain. *J. Mol. Biol.*, **294**, 373–387.
45. Kunz,C., Zurbriggen,K. and Fleck,O. (2003) Mutagenesis of the HMGB (high-mobility group B) protein Cmb1 (cytosine-mismatch binding 1) of *Schizosaccharomyces pombe*: effects on recognition of DNA mismatches and damage. *Biochem. J.*, **372**, 651–660.
46. Friddle,R.W., Klare,J.E., Martin,S.S., Corzett,M., Balhorn,R., Baldwin,E.P., Baskin,R.J. and Noy,A. (2004) Mechanism of DNA compaction by yeast mitochondrial protein Abf2p. *Biophys. J.*, **86**, 1632–1639.
47. Skoko,D., Wong,B., Johnson,R.C. and Marko,J.F. (2004) Micromechanical analysis of the binding of DNA-bending proteins HMGB1, NHP6A, and HU reveals their ability to form highly stable DNA-protein complexes. *Biochemistry*, **43**, 13867–13874.
48. Mukherjee,A., Sokunbi,A.O. and Grove,A. (2008) DNA compaction by histone-like protein HU from the hyperthermophilic eubacterium *Thermotoga maritima*. *Nucleic Acids Res.*, **36**, 3956–3968.
49. Ira,G., Malkova,A., Liberi,G., Foiani,M. and Haber,J.E. (2003) Srs2 and Sgs1-Top3 suppress crossovers during double-strand break repair in yeast. *Cell*, **115**, 401–411.
50. Biet,E., Sun,J.-S. and Dutreix,M. (1999) Conserved sequence preference in DNA binding among recombination proteins: an effect of ssDNA secondary structure. *Nucleic Acids Res.*, **27**, 596–600.